WP15ER-CPR(17) 16763

M. Chernyshova et al.

On some design aspects of the development of GEM Based Detectors for Plasma Diagnostics

Preprint of Paper to be submitted for publication in Proceeding of 2nd European Conference on Plasma Diagnostics (ECPD)

This work has been carried out within the framework of the EUROfusion Consortium and has received funding from the Euratom research and training programme 2014-2018 under grant agreement No 633053. The views and opinions expressed herein do not necessarily reflect those of the European Commission.

Development of GEM detector for plasma diagnostics application: simulations addressing optimization of its performance

M. Chernyshova[a,*], **K. Malinowski**[a], **E. Kowalska-Strzęciwilk**[a], **T. Czarski**[a], **P. Linczuk**[a,b], **A. Wojeński**[b] **and R. D. Krawczyk**[b]

[a] *Institute of Plasma Physics and Laser Microfusion, Hery 23, 01-497 Warsaw, Poland*

[b] *Warsaw University of Technology, Institute of Electronic Systems, Nowowiejska 15/19, 00-665 Warsaw, Poland*

E-mail: maryna.chernyshova@ipplm.pl

ABSTRACT: The advanced Soft X-ray (SXR) diagnostics setup devoted to studies of the SXR plasma emissivity is at the moment a highly relevant and important for ITER/DEMO application. Especially focusing on the energy range of tungsten emission lines, as plasma contamination by W and its transport in the plasma must be understood and monitored for W plasma-facing material. The Gas Electron Multiplier, with a spatial and energy-resolved photon detecting chamber, based SXR radiation detection system under development by our group may become such a diagnostic setup considering and solving many physical, technical and technological aspects. This work presents the results of simulations aimed to optimize a design of the detector's internal chamber and its performance. The study of the effect of electrodes alignment allowed choosing the gap distances which maximizes electron transmission and choosing the optimal magnitudes of the applied electric fields. Finally, the optimal readout structure design was identified suitable to collect a total formed charge effectively, basing on the range of the simulated electron cloud at the readout plane which was in the order of ∼2 mm.

KEYWORDS: Nuclear instruments and methods for hot plasma diagnostics; X-ray detectors; Electron multipliers (gas); Micropattern gaseous detectors (MSGC, GEM, THGEM, RETHGEM, MHSP, MICROPIC, MICROMEGAS, InGrid, etc.); Detector modelling and simulations.

* Corresponding author.

Contents

1. Introduction

The detection system based on Gas Electron Multiplier (GEM) technology [1] has been recently proposed as a soft X-ray (SXR) tomographic system for ITER-oriented tokamaks [2]. Thanks to its ability to discriminate energy and to determine spatial position of incoming X-rays, this technology is aimed to effectively monitor the impurity level of tungsten (chosen for the plasma facing material in ITER and future fusion reactor) in plasma. Such impurities degrade plasma performance, affect the behavior of plasma, and also, due to the interaction between particle transport and magnetohydrodynamic activity, might accumulate and lead to the most dramatic effect of W contamination - the so-called “radiative collapse”.

Detectors built based on GEM technology are expected to satisfy the main constraints on dimension, spatial position and required energy sensitiveness imposed on any X-ray detector for tokamak plasma in ITER and/or DEMO. In addition, combination of just two detectors would allow performing a poloidal tomography, an ultimate goal for plasma impurities transport studies. Such detection system is under development for some time through the collaboration between IPPLM (Poland), WUT (Poland) and CEA (France) aiming to be installed in a poloidal section of the WEST project tokamak [3], [4], [5], [6], [7]. This development has already required looking deeply into various aspects of design and performance of the detection system in general and of GEM detector in particular [8], [9], [10], [11], [12], [13]. This work focuses on the simulations of the most important detector parameters that affect its performance: electron transparency, ion feedback, electron cloud size and detector amplification. The effect of electrodes alignment was also researched to optimize the detector effectiveness as well as the finding of optimal electric field distribution through the detector.

2. Detector performance simulations

2.1 Motivation and methodology

The principle of GEM detector operation is based on collection of electron avalanches produced as a result of photoelectric effect, which is dominant for the SXR range for atomic gases. Triple-GEM detector consists of three GEM foils that are positioned in between the detector window and the readout plane. Such arrangement naturally creates four important structural parameters one need to identify when optimizing the internal geometry of a triple-GEM detector.

The **drift** or conversion **gap**, i.e. the first gap between the detector window and the first GEM foil must be adjusted to have: the drift velocity as high as possible, a high cluster density connected with small transverse drift velocity, high Townsend coefficient for a considerable amplification and low attachment coefficient. Overall, that should lead to fast dense pulses of the order of 20-50 ns on the readout plane.

Two **transfer gaps** (first and second) between consecutive GEM foils have to be as small as possible in order to obtain a fast charge transfer but keeping in mind existence of the electrostatic forces between two GEM foils and a possibility of a spontaneous discharge between two subsequent GEM foils.

Finally, the **induction gap** between the last GEM-foil and anode usually is minimized to produce the smallest possible induction area in order to deal with the fast readout schemes. However, a lower limit for the induction gap length exists (between 1 and 1.5 mm [14]) due to a possibility of having a discharge.

The modelling of electron motion in gas avalanche radiation detectors assists significantly in optimization as it allows testing range of designs under any (reasonable or not) values of internal and external parameters of operation. The standard procedure for such computer simulations was utilized in this paper. First, a spatial model of the detector cell was constructed together with finite elements mesh using Gmsh program [15]. Then, the three-dimensional map of the electric field distribution for the selected cell was obtained using Elmer FEM solver [16]. Finally, electron avalanche propagation is calculated in the whole detector structure solving the Boltzmann transport equations for electrons in gas mixtures under electric and magnetic fields using Magboltz [17] and Garfield++ [18].

Two kinds of simulations were done using the specified procedure. (1) Calculations of the electron avalanches for a single-GEM detector for four values of the electric field applied to the GEM foil and wide range of the electric fields above and below the foil. Based on the obtained results optimal values of the electric fields were chosen for the middle value of the GEM foil voltage applied, i.e. 380 V. (2) For the optimal electric field distributions found in (1), simulations of the triple-GEM detector electron avalanches were performed for different geometries of the detector electrodes. From the obtained data sets basic detector parameters, as electron multiplication coefficient, electron energy distribution, electron time distribution and radial distribution on readout plane were extracted.

2.2 Simulations of the detector parameters to optimize readout plane

The exemplary time distribution of the electron avalanche on the readout plane is shown in **Figure 1** for a triple-GEM detector of that specific arrangement. It could be seen that the readout electron signals are very fast lasting ~20 ns. The dominant effect on the time resolution is the time jitter derived from primary ionization. Because the primary ionization is a stochastic process governed by Poisson statistics, the drift time for a primary electron to reach the first GEM hole differs from event to event and thus, so does the initial time of the induced pulse on the readout electrode. Knowing that the time when the induced signal starts to develop is almost equal to the time needed to drift towards the GEM hole, knowing that the drift velocity is a function of the electric field and taking other requirements (such as parallax effect minimization, effective photon absorption, etc.) into account, the length of the drift gap can be estimated. Hereafter, in this paper all simulations were performed for 5 mm drift gap to achieve sufficient photo absorption efficiency at the level of 20% for 2-3 keV photons and ~20 ns of the pulse width.

The primary electrons cloud representing electrons originated in the drift gap forms an asymmetric drop-like shape while moving towards the first GEM foil as shown in **Figure 2 (a)**. That is related to a fact that overall charge distribution, i.e. with electrons *and* ions, has a drop like shape itself with fast moving electrons in the front and the slower ions at the back.

An example of the resultant electron cloud distribution on the readout plane, i.e. after going through the whole triple-GEM detector with the double conical holes GEM foils for the Ar/CO_2 70/30 gas mixture, is shown in **Figure 2 (b)**. Simulations of 100 of such electron avalanches (the results are shown in inset of **Figure 2 (b)**) showed that the total formed charge extends to ~2 mm spot. Based on this, the readout electrodes in the form of rectangular strips with 2.4 mm width were chosen for the final detector. Such width will allow both to collect almost the whole avalanche charge on the same strip (therefore minimizing the number of independent electronics channels) and not to compromise the accuracy of tomography (as the single tomographic line is sufficient to be less than 2.5 mm).

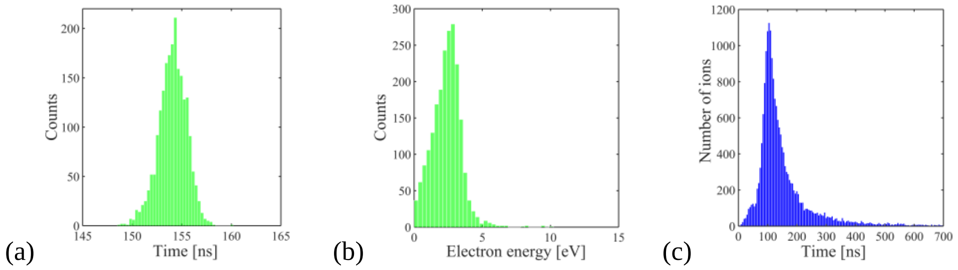

Figure 1. Triple-GEM arrangement 5/2/2/2 mm with 1500/700/700/900 V drift/transfer/transfer/induction voltages and with 360 V on each GEM foil: (a) Time distribution of the electrons reaching the readout plane with 0 ns being the time of the primary electron generation; (b) Energy distribution of the electron avalanche that reached the readout plane. Note that the energy of the electron avalanche is distributed around 2.4 eV; (c) Time distribution of the ions reaching the first GEM foil's upper electrode for 600/400/500/800 V and 380 V voltages.

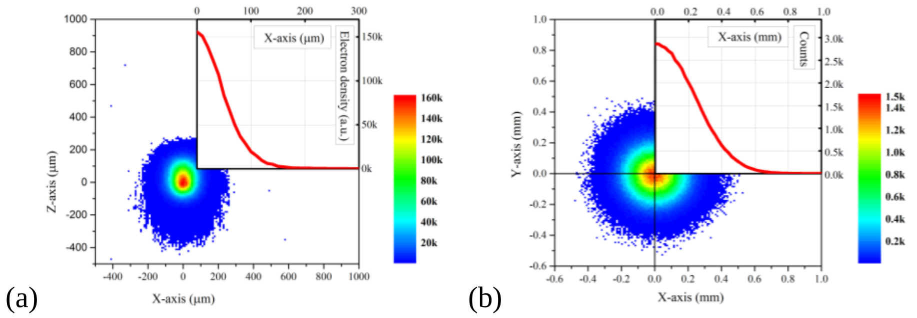

Figure 2. (a) Cross-sectional view of primary electrons cloud forming a drop-like shape where positive values of Z-axis point towards the first GEM foil. The calculations were performed for electrons originated from 5.9 keV photons interacting with Ar/CO_2 70/30 gas mixture at 1500 V drift voltage. Notice the size of a drop-like shape in Z-direction is almost 1.5 times bigger than in X/Y-directions. (Inset shows the electron density as a function of X for Z=0). (b) Top view of the electron cloud on the readout plane. The calculations were performed for 5/2/1/2 mm arrangement for 1500/700/700/800 V drift/transfer/transfer/induction voltages and with 380 V on each GEM foil. (Inset shows the counts of electrons collected from 100 electron avalanches as a function of a distance from the cloud center).

2.3 Simulations of the detector parameters addressing optimization of its performance

The overall performance of the detector was assessed as a function of the drift (above the first GEM electrode) and transfer (below the second GEM electrode) electric field values. Four basic characteristics were extracted representing different aspects of the performance: $\boldsymbol{P_1}$, number of ions landed on the upper copper GEM foil electrode normalized to the total number of ions; $\boldsymbol{P_2}$, the ratio of the electrons reached the readout plane to the all generated primary electrons, i.e. gain; $\boldsymbol{P_3}$, electron transparency expressed as percentage of starting electrons that get to the holes and are multiplied; and $\boldsymbol{P_4}$, electron transport efficiency expressed as the number of electrons on readout to the total number of electrons produced during avalanche propagation. Based on these parameters, an "average optimum coefficient" was proposed having the following expression: $\boldsymbol{P_{opt} = P_1/P_{1max} \cdot P_2/P_{2max} \cdot P_3/P_{3max} \cdot P_4/P_{4max}}$. The results are presented in **Figure 3** together with the results of the electron multiplication simulations for the studied gas mixture as a function of the applied electric field. As it could be observed, electron amplification starts to rise over 700 V/cm.

Based on the obtained values of the optimized parameter $\boldsymbol{P_{opt}}$ and taking into account that electrons begin to multiply when the field is over 5000 V/cm (see **Figure 3**), the following electrical field values identify the voltage selection for the optimal triple-GEM detector: 1200 V/cm in the drift gap, 2000 V/cm in the first transfer gap, 2500 V/cm in the second transfer gap, and 4000 V/cm in the induction gap (summarized as 1200/2000/2500/4000 V/cm set). **Table I** presents the values of voltages and the values of basic characteristic parameters for triple-GEM detectors with different spacing using this set of electric fields.

In order to confirm the prediction, additional simulations of signals (from 209 primary electrons – an average value of created electrons by a ^{55}Fe source photon absorption) were performed for the triple GEM-detector with the 5/2/2/2 mm configuration. Besides an optimized set of 600/400/500/800 V (see **Table I**), the sets of 1500/700/700/900 V and 950/600/700/1000 V

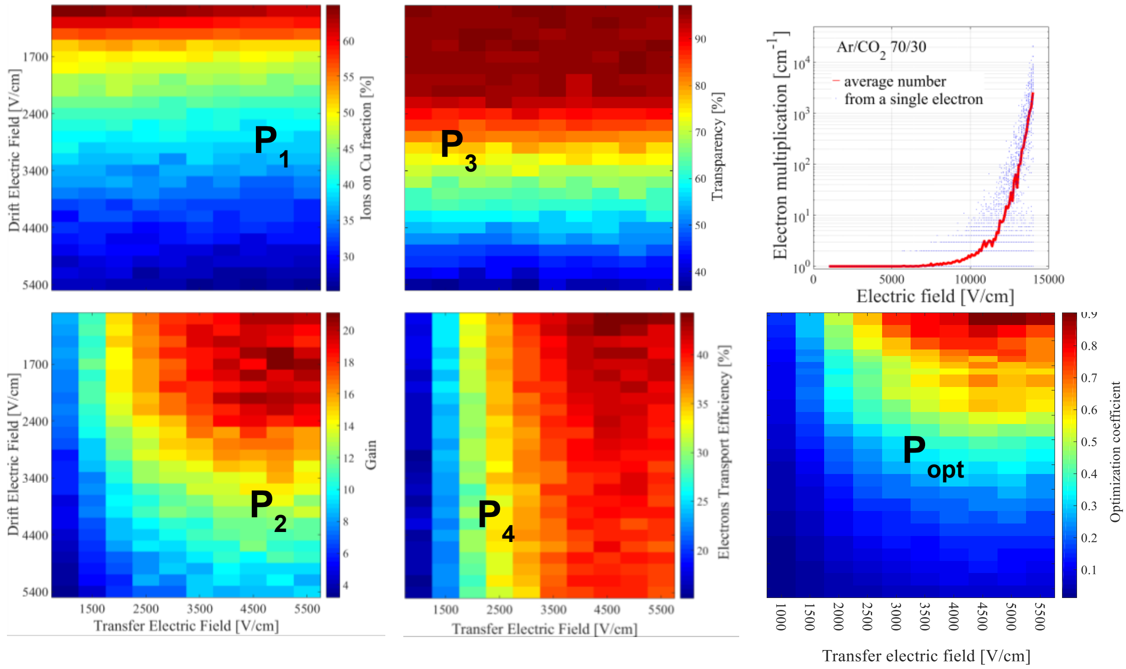

Figure 3. 2D maps of basic calculated characteristics P_1, P_2, P_3, P_4 as well as an optimized parameter P_{opt} that represents the overall detector electric field distribution as a function of the drift (above the first GEM electrode) and transfer (below the second GEM electrode) electric field values. Number of generated electrons as a function of the electric field magnitude simulated using Garfield++ for Ar/CO_2 70/30.

Table I. The calculated values of basic characteristics P_1, P_2, P_3, and P_4 for different structures with voltages obtained using 1200/2000/2500/4000 V/cm optimized set of electric fields.

Spacing [mm]	Voltage [V]	P_1 [%]	P_2 [gain]	P_3 [%]	P_4 [%]
5/1/1/1	600 / 200 / 250 / 400	56.00	4354	65.28	41.59
5/1/1/2	600 / 200 / 250 / 800	55.08	5673	66.24	42.30
5/1/2/1	600 / 200 / 500 / 400	55.44	4584	66.57	41.01
5/1/2/2	600 / 200 / 500 / 800	55.30	4862	65.28	41.77
5/2/1/1	600 / 400 / 250 / 400	53.76	5040	65.31	41.41
5/2/1/2	600 / 400 / 250 / 800	53.50	5156	65.29	42.13
5/2/1/3	600 / 400 / 250 / 1200	54.46	4306	66.60	41.19
5/2/2/1	600 / 400 / 500 / 400	53.28	4583	65.61	41.08
5/2/2/2	600 / 400 / 500 / 800	55.89	4771	65.27	41.83
5/3/1/2	600 / 600 / 250 / 800	53.87	5399	66.88	42.24
5/3/3/3	600 / 600 / 750 / 1200	49.73	5202	66.84	41.08

were used. The results (not presented here) confirm that the optimized values produces an approximately 50% higher gain.

All values of basic characteristics presented in **Table I** are quite close to each other except the values calculated *not* for the optimized set of 1200/2000/2500/4000 V/cm. The final choice of spacing for a detector to be built therefore, has to be performed based on other information, requirements and/or limitations. Choice of 1 mm spacing for either or both transfer gaps implies difficulty of positioning GEM foils so close to each other. Nevertheless, two spacing configurations could be further investigated for the triple-GEM detector under construction: 5/1/1/2 and 5/3/1/2 mm.

3. Summary

This work presents the results of simulations aimed to optimize the detector's internal chamber and performance. The modelling of electron motion in gas avalanche radiation detectors was conducted for the range of values of internal and external parameters of operation. The analysis of the detector's performance was based on electron multiplication coefficient, electron energy distribution, electron time distribution, radial distribution on readout plane and other useful parameters. The following set of electrical field values was identified as the optimal for a triple-GEM detector: 1200/2000/2500/4000 V/cm for drift/transfer/transfer/induction gaps, respectively. Suitability of the triple-GEM detectors with the 5/1/1/2 and 5/3/1/2 mm spacing and rectangular readout electrodes with 2.4 mm width to act as a first detector chamber design for the SXR measurements of plasma radiation will be justified.

Acknowledgments

This work was partly supported by Polish Ministry of Science and Higher Education within the framework of the scientific financial resources in the years 2014-2017 allocated for the realization of the international co-financed project. This work has been carried out within the framework of the EUROfusion Consortium and has received funding from the Euratom research and training programme 2014-2018 under grant agreement No 633053. The views and opinions expressed herein do not necessarily reflect those of the European Commission.

References

[1] F. Sauli, *The gas electron multiplier (GEM): Operating principles and applications*, *Nucl. Instr. Meth. A* **805** (2016) 2.

[2] D. Vezinet et al., *Fast nickel and iron density estimation using soft X-ray measurements in Tore Supra: preliminary study*, *Fusion Sci. Technol.* **63** (2013) 9.

[3] M. Chernyshova et al., *Development of GEM gas detectors for X-ray crystal spectrometry*, *JINST* **9** (2014) C03003.

[4] M. Chernyshova et al., *Conceptual design and development of GEM based detecting system for tomographic tungsten focused transport monitoring*, *JINST* **10** (2015) P10022.

[5] T. Nakano et al., *Determination of tungsten and molybdenum concentrations from an X-ray range spectrum in JET with the ITER-like wall configuration*, *J. of Physics B: At. Mol. Opt. Phys.* **48** (2015) 144023.

[6] M. Chernyshova et al., *Development of GEM detector for tokamak SXR tomography system: Preliminary laboratory tests,* Fusion Eng. Des. (2017) [`https://doi.org/10.1016/j.fusengdes.2017.03.1072017`].

[7] M. Chernyshova et al., *Gaseous electron multiplier-based soft X-ray plasma diagnostics development: preliminary tests at ASDEX Upgrade*, *Rev. Sci. Instrum. 87 (2016) 11E325*.

[8] M. Chernyshova et al., *GEM detector development for tokamak plasma radiation diagnostics: SXR poloidal tomography*, *Proc. SPIE* **9662** (2015) 966231.

[9] S. Jednorog et al., *Results of neutron irradiation of GEM detector for plasma radiation detection*, *Proc. SPIE* **9662** (2015) 96622Y.

[10] G. Kasprowicz et al., *Readout electronics for the GEM detector*, *Proc. SPIE* **8008** (2011) 80080J.

[11] A. Wojenski et al., *Diagnostic-management system and test pulse acquisition for WEST plasma measurement system*, *Proc. SPIE* **9290** (2014) 929029.

[12] A. Wojenski et al., *Multichannel measurement system for extended SXR plasma diagnostics based on novel radiation-hard electronics*, *Fusion Eng. Des. (2017)* [`https://doi.org/10.1016/j.fusengdes.2017.04.134`].

[13] T. Czarski et al., *Data processing for soft X-ray diagnostics based on GEM detector measurements for fusion plasma imaging*, *Nucl. Instr. Meth. B* **364** (2015) 54.

[14] S. Bachmann et al., *Discharge studies and prevention in the gas electron multiplier (GEM)*, *CERN-EP/2000-151, 11 December 2000*.

[15] C. Geuzaine et al., *Gmsh: a three-dimensional finite element mesh generator with built-in pre- and post-processing facilities*, *Int. J. Numer. Meth. Eng.* **79** (2009) *1309*.

[16] C.I.C. for Science, *Elmer: Open Source Finite Element Software for Multiphysical Problems*, [`http://www.csc.fi/english/pages/elmer`].

[17] S. F. Biagi, *Monte Carlo simulation of electron drift and diffusion in counting gases under the influence of electric and magnetic fields*, *Nucl. Instr. Meth. A* **421** (1999) 234.

[18] R. Veenhof, *Garfield - simulation of gaseous detectors*, [`http:://cern.ch/Garfield`].